

AC - conductivity studies on $Y_{1-x}Bi_xCrO_3$ solid solution

Venkateswara Rao Mannepalli and Ranjith Ramadurai

Citation: [AIP Conference Proceedings](#) **1832**, 110017 (2017); doi: 10.1063/1.4980641

View online: <http://dx.doi.org/10.1063/1.4980641>

View Table of Contents: <http://aip.scitation.org/toc/apc/1832/1>

Published by the [American Institute of Physics](#)

AC - Conductivity Studies On $Y_{1-x}Bi_xCrO_3$ Solid Solution

Venkateswara rao Mannepalli and Ranjith Ramadurai*

*Department of Material Science and Metallurgical Engg.
Indian Institute of Technology Hyderabad, Kandi, Sanga reddy, Telangana, 502285,
India. *Corresponding author: ranjith@iith.ac.in.*

Abstract. $YCrO_3$ and the substitution of $Bi^{+3}(6s^2)$ in the Y-site were synthesized by the sol gel process. The conductivity measurements using dielectric spectroscopy reveals that conductivity increases with increase of composition. Dielectric loss were used to understand the nature of conducting species and it reveals that chromates exhibits the usual reciprocal behaviour of charge carriers to motion of oxygen vacancies as we increase the Bi composition and temperature. Impedance and microstructural studies revealed that conductivity of the chromates was dominated by the grain contribution.

Keywords: Sol gel, Impedance spectroscopy, ac-conductivity.

PACS:

INTRODUCTION

Multiferroics are materials with simultaneous existence of electric and magnetic ordering. They are fundamentally significant and have been proposed for wide range of applications¹. Chromites ($LnCrO_3$ where Ln =lanthanides or Yttrium) are extensively studied for different applications like interconnect of solid oxide fuel cells, gas sensors, humidity sensors, Negative temperature coefficient (NTC) thermistors etc.^{2,3,4}. But observation of ferroelectric relaxor behaviour in $YCrO_3$ (YCO) stirred the research in different direction in chromites⁵. YCO was observed to possess local structural distortions with lower symmetry which is expected to exhibit ferroelectric properties⁶. Due to leakage currents of chromites measurement of ferroelectric polarization is inhibited in YCO⁷. In this study, we aim to understand conduction mechanism through impedance spectroscopy in YCO and Bi substituted $Y_{1-x}Bi_xCrO_3$ (YBiCO).

EXPERIMENTAL

$Y_{1-x}Bi_xCrO_3$ ($x=0, 0.05, 0.1$ and 0.15) was prepared by sol gel route using nitrates of yttrium, chromium and bismuth. The obtained powders were calcined at 1123K for 4hrs and further pelletized in the form of circular disc size 6 mm diameter and 1 mm thickness. The green pellets were heat treated at 773K for 1h at the rate of 5K/ min in order to remove the binder and then finally sintered at 1373K for 10h at the rate of 5K / min. X-Ray Diffraction (XRD) was performed by collecting the data from Panalytical X'pert Pro X-ray

diffractometer with $Cu K_{\alpha}$ radiation ($\lambda=1.5406 \text{ \AA}$) as a source. Dielectric properties are measured by using Wayne Kerr 6500B impedance analyzer with in a frequency from 100Hz to 1MHz. Electroding of the sintered samples by using silver paint and curing was done for 1hr at 473K. Measurements were carried from room temperature (RT~303K) to 573K.

RESULTS AND DISCUSSION

Diffraction studies on $Y_{1-x}Bi_xCrO_3$ ($x=0$ to 0.15) compounds are well refined with the orthorhombic $Pnma$ structure without any impurity at room temperature, reported elsewhere⁸. Increase of lattice parameters, volume expansion and increase of Cr-O2-Cr bond angles are consistent with Bi^{+3} ($r=1.11\text{\AA}$) in Y^{+3} -site ($r=1.02 \text{ \AA}$). Frequency dependent dielectric studies are carried at different temperatures within 100Hz to 1MHz frequency range. Field Emission scanning electron Microscopy images were taken using gold electroding on the surface. Present paper will discuss about Impedance measurements of the YCO ($x=0$) and $Y_{0.85}Bi_{0.15}CrO_3$ ($x=0.15$). Frequency dependent ϵ' and ϵ'' where ϵ' the real part and ϵ'' the imaginary part of electrical permittivity revealed that there was increase of ϵ'' with decrease of frequency. The increase of ϵ'' at low frequencies reveals that conduction mechanism plays a very important role in our samples. In order to understand the conduction mechanism we plot the ac conductivity calculated from the following Eq (1) with different temperatures

and frequency are plotted for x=0 and 0.15 as shown in Fig 1.

$$\sigma_{ac} = \epsilon' \epsilon_0 \omega \tan \delta \dots\dots\dots (1)$$

Where ϵ_0 permittivity of free space, ω is angular frequency and $\tan\delta$ is dielectric loss. The strong rise of conductivity with frequency is observed in x=0 at low temperatures and as temperature increases we observe plateau region in YCO from 313K to 553K. In x=0.15 the plateau region at low frequencies and strong rise of conductivity at high frequencies is observed. With temperature we observe more plateau region, dc conductivity, for x=0.15. This reveals that conduction mechanism with different composition at different frequencies is different. The strong rise of conductivity behaviour observed at low frequencies is due to grain boundary effect⁹ in parent or pristine samples. dc conductivity in x=0.15 at low temperatures and frequencies may be combined effect of grain and grain boundary.

Temperature dependent ac conductivity at 1MHz is shown in Fig 2. Linear relationship maintains at higher temperatures (>523K) and nonlinearity observed at lower temperatures. The linear regions are fitted with the arrhenious relationship and obtained activation energies of 0.21eV and 0.7eV for x=0 and x=0.15 compositions respectively. The conductivity in YCO samples is attributed to small polaron created by the local structural distortions¹⁰.The conductivity in x=0.15 at high temperature (>523K) based on activation energies revealed that presence of oxygen vacancies or defects^{9, 11}. The conductivity at low temperatures in x=0.15 shows a nonlinear behaviour whose conduction mechanism is entirely different from the pristine compound.

From frequency dependent dielectric loss we can understand the nature of conductive species¹² by using Eq (2)

$$\epsilon'' = B(T). \omega^s \dots\dots\dots (2)$$

B (T) temperature dependent parameter and 's' reveals the behaviour of charge carriers. The log-log scale for ϵ'' vs. ω is shown in Fig 3(a) at 533K for x=0 and 0.15. For x=0 we observed straight line fitting and obtained 's' value is close to -1 which indicates the conduction is due to the charge carriers that has an inverse relation similar to dielectric relaxation with frequency. Thus the conductivity due to small polaron is interrelated to observed dielectric relaxation in YCO samples. In x=0.15 at higher frequencies we observe a deviation from straight line whose conduction mechanism is different compared to the lower frequencies. This reveals that there are more than one conduction mechanism responsible for x=0.15 compounds. The different values of 's' obtained from different slopes with temperature reveals that conduction mechanism is

not same throughout temperature in x=0.15. Microstructural images shown in Fig 3 (b) & (c) reveal that there is increase of grain size with increase of Bi composition. Thus possible conduction in x=0.15 sample is due to both within the grain and grain boundary contributions.

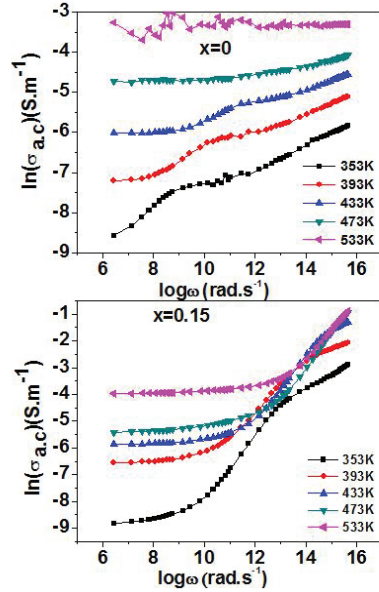


FIGURE 1. A.C conductivity measurements at different temperatures for x=0 and 0.15. Plateau region indicates DC conductivity

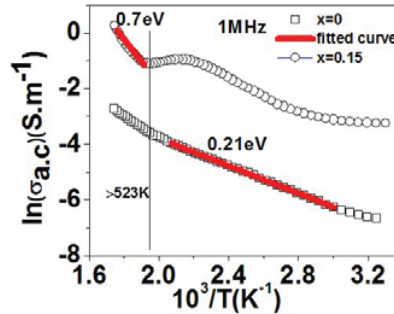


FIGURE 2. A.C conductivity measurements with temperature at 1MHz and linear fits with activation energies.

Further we employed plots of imaginary part (Z'') versus real part (Z') of impedance. Nyquist (Z'' vs Z') shown in Fig 4) diagrams are used to understand the conduction contribution from grain or grain boundaries. The apex of the semicircle reveals the relaxation frequency which will be used to distinguish from bulk or grain to grain boundary. The experimental points are well fitted with the two parallel R-C (constant phase element, CPE) circuits in series and the corresponding high frequency resistance (R_1) and

capacitance (CPE_1) are related to grain contribution whereas low frequency resistance (R_2) and capacitance (CPE_2) are effect of grain boundary contributions.

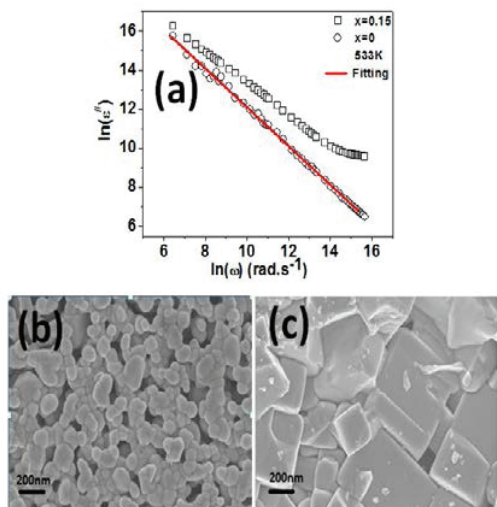


FIGURE 3. (a) Log scale plots for ϵ'' versus ω (b) microstructural images of $x=0$ & (c) $x=0.15$

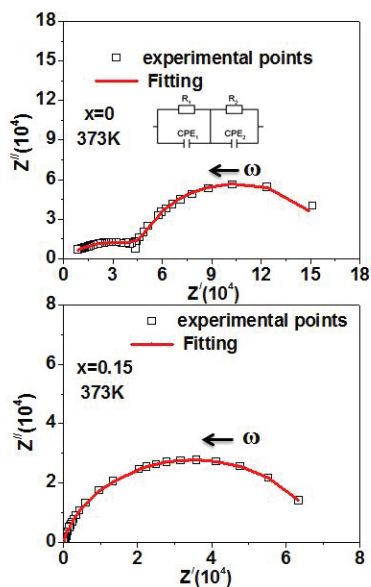


FIGURE 4. Z'' vs Z' for $x=0$ and 0.15 at $373K$

The observed resistance values for high frequency circle decreases with increase of composition. The decrease of grain boundary resistance with temperature (373-453K) from 55K Ω to 9K Ω and 67K Ω to 11K Ω for $x=0$ and 0.15 respectively. The decrease of grain resistance with temperature from 1M Ω to 4K Ω and 956 Ω to 54 Ω for $x=0$ and 0.15 respectively. This reveals that conduction in $x=0.15$ at low frequencies is

combined effect of grain and grain boundary whereas at higher frequencies the creation of oxygen vacancies and their motion leads to increase of conductivity at higher temperatures.

Thus the ac conductivity, frequency dependent dielectric loss and Impedance measurements reveal that there is increase of conductivity with increase of composition. The conduction mechanism in pristine samples is due to small polaron formed due to local structural distortion in support to the obtained activation energies. The high activation energies observed in substituted samples at higher temperatures reveals that conduction is due to motion of oxygen vacancies. The nonlinear conductivity at low temperature reveals that conduction mechanism in $x=0.15$ is combined effect of grain and grain boundary. Impedance and microstructural studies support the observed conductivities in $x=0$ and $x=0.15$ are dominated by the grain.

ACKNOWLEDGMENTS

Authors would like to acknowledge the MHRD Govt of India and DST No.SERB/F/5142/2013-14/ for financial support.

REFERENCES

- Sang Wook Cheong and Maxim Mostovoy *Nat. Mater.* **6**, 13–20 (2007).
- San ping jiang *Int. J. Hydrogen Energy* **37**, 449-470 (2012).
- Minh N.Q *J. Am. Ceram. Soc.* **76**,563-588 (1993).
- A.Nguetou kamlo, J.Bernard, C.lélievre, D.Houivet *J. Eur. Ceram. Soc.* **31**, 1457-1463 (2011).
- C.R.Serrao, A.K.Kundu, S.B.Krupanidhi, U.V.Waghmore and C.N.R Rao *Phys. Rev. B* **72**, 220101(R) (2005).
- K. Ramesha, A Llobet, Th. Proffen, C. R. Serrao, and C. N. R. Rao *J. Phys. Condens. Matter.* **19**, 102202 (2007).
- B.Rajeswaran, D. I. Khomskii, A. K. Zvezdin, C. N. R. Rao and A. Sundaresan *Phys.Rev.B* **86**, 214409 (2012).
- Venkateswara rao Mannepalli and Ranjith Ramadurai *MRS Advances I*, 609-614 (2016).
- M.A.L. Nobre and S.Lanfredi *J.Appl.Phys* **93**, 5576 (2003).
- A.Duran, E.Verdin, R.Escamilla, F.Morales and R.Escudero *Mat.Chem.Phys.* **133** 1011-1017 (2011).
- M.A.L Nobre and S.Lanfredi *Appl. Phys.Lett* **81**, 453 (2002).
- C.C.wang, C.M.Lei, J.wang, X.H.Sun, T.Li, S.G Huang, H.wang and Y.D.Li *J.Appl.Phys* **113**,094103 (2013).